Geometric phases in soft materials

Abbaszadeh, H.

Chapter 1.

Introduction

Geometric phases are *extra* phase factors (additional to the dynamical ones, i.e. integral of system's energy over time), that are acquired by moving along a closed -adiabatic- path [147, 161] in the parametric space of a given Hamiltonian. The use of the term geometric here stems from the fact that this phase depends on the path taken in the phase space, and not for example on the rate of moving along that path. Consider for example the quantum mechanical wavefunction of an electron which is described in terms of an amplitude a and a phase ϕ as $\psi(\mathbf{r}) = ae^{i\phi}$. After switching on a magnetic field, the electron's wavefunction is modified into $\psi(\mathbf{r}) = ae^{i\phi - ie\mathbf{A}\cdot\mathbf{r}}$, where e is the electrical charge, and $\mathbf{A}$ is the vector gauge field. (Throughout this thesis we set $\hbar = 1$.) Now, consider the movement of this electron on a cyclic path in space, denoted by $\mathcal{C}$: while the amplitude remains intact, the wavefunction acquires a phase

$$\Phi = -e \oint_{\mathcal{C}} \mathbf{A} \cdot d\mathbf{r}, \tag{1.1}$$

which is equal to the total magnetic flux inside the region that is enclosed by $\mathcal{C}$. This effect is independent of whether the electron experiences the magnetic field directly, especially when the magnetic field is confined in a region, this phase is independent of the path taken by the electron surrounding that region. This fundamental feature of quantum mechanics is the essence of the Aharonov-Bohm effect [185], see Fig. 1.1(a).

The notion of geometric phases was independently developed in the context of electromagnetic waves by Pancharatnam [186] and in the adiabatic Hamiltonian evolution in quantum mechanical systems by Berry [155, 161] as a more general concept. Later on, Hannay used the same mathematical

concept for classical systems [160]. The Hannay angle, which is the geometric phase that, for instance, makes the Foucault pendulum precess, is an example of how a geometric concept in quantum mechanics can lead to a new frame of looking at a classical problem. One of the tasks of this thesis is to follow a similar passage by adopting an already existing concept (usually formulated in an electronic or cold atom language) to a classical, soft matter platform.

When considering the broadness of a subject and its applicability, Berry's formulation of the quantum adiabatic phase has proven to be a very fruitful discovery of theoretical physics in the past few decades. The range of phenomena that involves this phase spans from the quantum Hall effect [153, 157, 166, 169, 170] and topological insulators [96, 100] to classical mechanics [159, 160], to optical fibers [134, 155, 186], and the rotation of a cat when falling from a height [148]. The geometrical phases are usually measured through interference experiments: the geometrical phases that are acquired by a wavefunction are different when moving along different paths in the parametric space. In the example above, this was done by the interferometry between the electrons that traverse different paths[183, 185].

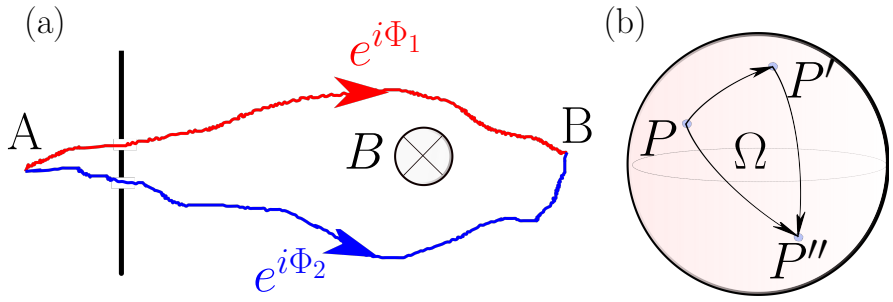

Figure 1.1: (a) The Aharanov-Bohm effect. An electron acquires different phases when its quantum mechanical paths encircle a region that contains a magnetic field. The phase difference $\Phi = \Phi_1 - \Phi_2$ is equal to the total magnetic flux multiplied by electron's electric charge and is unchanged under the smooth deformations of the paths. (b) Light polarization represented on a Poincaré sphere. Similar to the Aharanov-Bohm effect for electrons, the change in the polarization is non-transitive and after traversing a loop, the light beam acquires a geometrical Pancharatnam-Berry phase equal to $\Omega/2$, where Ω is the solid angle that is enclosed by this loop on the Poincaré sphere.

We shall now review the Berry phase and its relation to the field of topological insulators among other applications.

1.1 Adiabatic theorem and the Berry phase

In quantum mechanics, where the dynamics of a system's wavefunction is described by the Schrödinger equation,

$$i\partial_t |\psi\rangle = H |\psi\rangle , \tag{1.2}$$

the adiabatic theorem states that a system that is in one of its eigenstates continues to stay in that state as long as the changes in the Hamiltonian occur slowly enough compared to the energy gap between the corresponding eigenenergy of this state and the rest of the spectrum [45]. Let us then consider the case of a Hamiltonian that evolves along a cyclic adiabatic path in a parameter space, that we represent by a vector $\boldsymbol{\lambda}(t)$ [♠]. The adiabatic theorem above ensures that upon completion of a loop in this parametric space, the system will be in the same quantum eigenstate as the one it started from. This can be represented as $\psi_n(t) = e^{i\gamma_n}\psi_n(t_0)$, where γ_n is a phase that is acquired along the evolution, n denotes the eigenstate index, and t_0 and t are the initial and final time.

Berry showed that apart from a trivial dynamical contribution

$$\gamma_{\text{dyn}} = -\int_{t_0}^{t} \nabla_{\boldsymbol{\lambda}} E_n(\boldsymbol{\lambda}(t)) \cdot \frac{d\boldsymbol{\lambda}}{dt} dt, \tag{1.3}$$

the phase γ_n has a second nontrivial part that is related to the geometric features of the cyclic path of the Hamiltonian in the parameter space. The Berry phase is defined by

$$\gamma_{\text{geom}} = -\oint_{\mathcal{C}_{\boldsymbol{\lambda}}} \mathcal{A}_n(\boldsymbol{\lambda}(t)) \cdot d\boldsymbol{\lambda} \tag{1.4}$$

as the integrand of the Berry connection

$$\mathcal{A}_n(\boldsymbol{\lambda}) = -i \langle \psi_n(\boldsymbol{\lambda})| \nabla_{\boldsymbol{\lambda}} |\psi_n(\boldsymbol{\lambda})\rangle \tag{1.5}$$

over the cyclic path $\mathcal{C}_{\boldsymbol{\lambda}}$ in parameter space. Note the resemblance between this definition and Eq. 1.1. In fact, this similarity in the structure is not accidental, but rather suggests that the Berry connection stems from a gauge freedom [152] that is arising from the invariance of a theory under a gauge transformation $|\psi\rangle \to e^{i\alpha(\boldsymbol{\lambda})} |\psi\rangle$. Here, such a transformation leads to $\mathcal{A}_n(\boldsymbol{\lambda}) \to$

[♠] These control parameters are usually tuned through an external mechanism, such as by inducing an electromagnetic field, or shining light to the system. As we will see later on, it can also represent the Bloch momentum in the Fourier space.

$\mathcal{A}_n(\boldsymbol{\lambda}) + \nabla_{\boldsymbol{\lambda}}\alpha$ and, therefore, the loop integral in Eq. 1.4 is invariant under this transformation using the Stokes' theorem:

$$\gamma_{\text{geom}} = -\int_{\mathcal{S}} \mathcal{F} d^2\boldsymbol{\lambda}, \tag{1.6}$$

where $\mathcal{F}_{ij} = \dfrac{\partial \mathcal{A}_i}{\partial \lambda^j} - \dfrac{\partial \mathcal{A}_j}{\partial \lambda^i}$ is called the Berry curvature and $\mathcal{S}$ is the interior region of $\mathcal{C}_{\boldsymbol{\lambda}}$ in the parameter space. (We dropped the state index n for the sake of simple notations.) There is a fundamental difference between γ_{dyn} and γ_{geom}. The former is rate dependent: one can stay at the same point in the parameter space and still acquire a dynamical phase, whereas the adiabatic phase is merely determined by the geometrical structure of the eigenmodes associated with the loop $\mathcal{C}_{\boldsymbol{\lambda}}$.

1.1.1 Topology and geometric phases

We saw above that the adiabatic phase has a geometric nature. For example, when measured *locally* (by narrowing down the loop so that $\mathcal{S}$ is an infinitesimally small region in the parameter space), it can determine the Berry curvature on a smooth manifold. This phase is an example of a more general differential geometry concept called holonomy [167]. Let us see how this works in a real-life situation. Consider the cyclic path of a motorcycle on a wall of death in such a way that the initial and final positions coincide. It is then imaginable that the initial and final states of the motorcycle plus the cyclist are the same, except maybe some effects of time-dependent dynamical nature (the petroleum level being reduced, internal states of the cyclist and the motorcycle is changed, etc.). Note also that this lack of the geometric phase does not also depend on the path taken between the initial and final points. Now, imagine this experiment is done on a Möbius strip, as shown in Fig. 1.2(c) ♠. We can see that this time the final state of the motorcycle and the cyclist is flipped with respect to their initial state by gaining a geometric phase π. Again, this geometric phase is independent from the intermediate path that is taken between the initial and final points.

This is an example of a holonomy that is dependent on a *global* geometric character of a manifold that is determined by its topology. To affect such topological characteristics, one needs to consider discontinuous changes in the shape of the manifold, such as the one is shown by Fig. 1.2(b).

♠This is not recommended in a real world situation, since some positive curvature is in play!

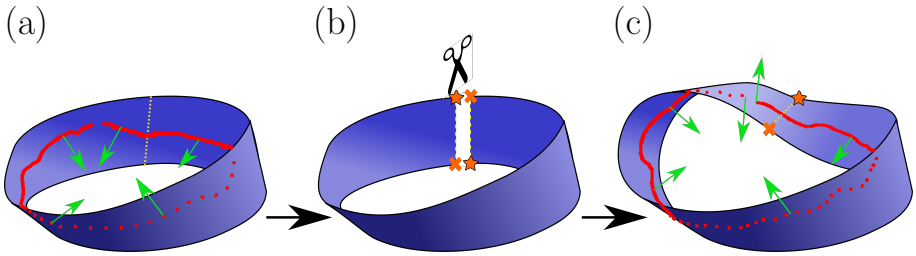

Figure 1.2: A Möbius strip can be obtained from a cylindrical object by a non-continuous deformation, as in (b). The difference between topology of the initial, (a), and final, (c), objects can be shown by tracking a director field on a loop and find the difference in its orientation between the initial and final states.

A fruitful result of Berry's geometric phases was its role in the development of topological modes which led to an explanation of the quantized Hall conductance in the quantum Hall effect [170]. While discussing this connection in full detail and in its rigorous mathematical formalism is beyond the scope of this introduction, it is worthwhile to see how this fascinating subject of modern physics was rooted in the geometric phases which we discussed above.

Let us consider a general Hamiltonian that is invariant under a translation operator. The eigenmodes of such a Hamiltonian will be Bloch waves $\psi_k(x) = u(x)e^{ikx}$, where $u(x)$ is a periodic function and k is a wavenumber that belongs the a periodic region in the reciprocal space that is called the first Brillouin zone (BZ). The eigenenergies of the system can be derived by diagonalizing the Fourier transformed Hamiltonian $H(k)$ for each wavenumber. This calculation results in a set of continuous bands of energies in the BZ, constructing the band structure of H. This procedure can be formulated as below: For each Hamiltonian $H(x)$ on a periodic boundary condition, there exists a set of Fourier transformed (Bloch) Hamiltonians $H(k)$ that are parametrized by a wavenumber $k \in 1^{st}$ BZ. Hence, if the band structure of H is gapped, one can apply the adiabatic theorem to calculate the Berry phase of the nth band on the momentum space

$$\gamma_n = i \oint_{1^{st}\ \mathrm{BZ}} \langle \psi_n(\mathbf{k}) | \nabla_{\mathbf{k}} | \psi_n(\mathbf{k}) \rangle \cdot d\mathbf{k} \tag{1.7}$$

where $|\psi_n(\mathbf{k};t)\rangle$ is the n-th eigenstate of the Hamiltonian and $\mathbf{k}$ is the adiabatic parameter. The integral in the right hand side is related by Stoke's theorem to the integral of the Berry curvature, $\mathcal{F} = \nabla \times \mathcal{A}$, where $\mathcal{A}$ is the Berry connection, as defined by Eq. 1.5 in the reciprocal space. The later integral is related to the first Chern number through [187]

$$C = \frac{1}{2\pi} \int \mathcal{F} d^2\mathbf{k}, \tag{1.8}$$

which is an integer number and is the one that was used by TKNN [169] to explain the quantization of the quantum Hall conductivity which was observed by von Klitzing [170] ♠.

1.2 Geometric phases in classical systems

Geometric phases are not quantum effects. Hannay formulated them in the context of classical Hamiltonian systems [150, 160]. For example, such geometric phases lead to the precession of a pendulum in a rotating frame. Another example is in the context of light polarization dynamics, which was discovered by Pancharatnam a few decades before Berry's adiabatic phase. A monochromatic light wave with a wavevector $\mathbf{k}$ and frequency ω that travels along a fixed direction acquires a dynamical phase

$$\Phi_{\text{dyn}} = e^{i\mathbf{k}\cdot r - i\omega t}. \tag{1.9}$$

However, this contribution does not consider a polarization degree of freedom which adds a vectorial nature to the state of the light wavepacket, for example when it passes through a polarizer. The polarization can be represented by a complex vector on a Poincaré (or Bloch) 2-sphere. Passing through a polarizer, which we show by $[P \to P']$ in the example above is then represented by a geodesic path between two polarization states on the Poincaré sphere, as shown by Fig. 1.1(b).

Pancharatnam showed that such phases acquired by the light beam are non-transitive, i.e. $[P \to P'] \cup [P' \to P''] \neq [P \to P'']$ and the difference is given by the half of the solid angle of the closed loop between these three points [186], namely

$$\Phi_{\text{geom}} = \frac{1}{2}\Omega_{PP'P''}, \tag{1.10}$$

♠Notice that this sentence is describing two Nobel physics prizes!

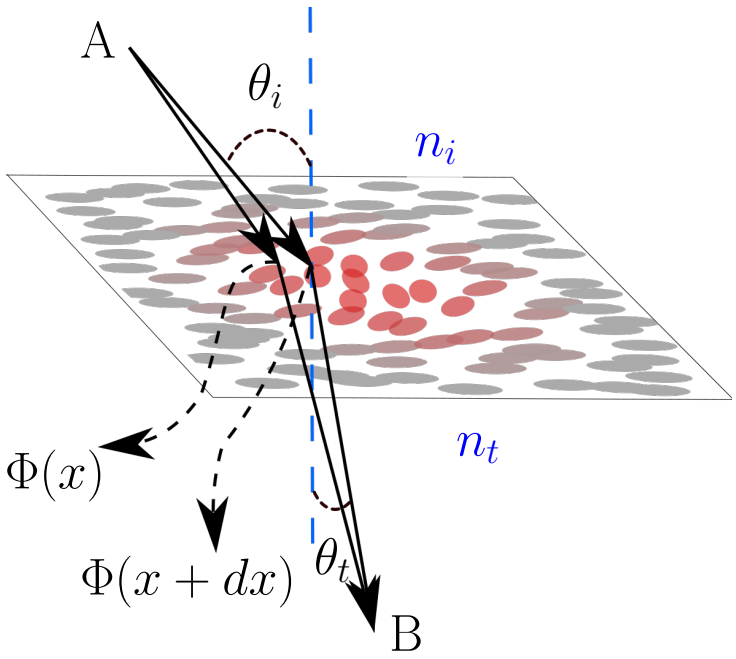

Figure 1.3: Generalized Snell's law, after Ref. [98].

see Fig. 1.1(b). Once again, it is important to note that this phase is not the same as the regular dynamical phase that the light beam acquires along its evolution. Rather, it is an extra phase that is merely determined by the geometry of the path that is taken by the polarization state of light on the Poincaré sphere. This phase is equivalent to the adiabatic phase on the Bloch sphere of a an electron in a magnetic field, similar to the Aharonov-Bohm experiment [155]. This means that the Pancharatnam phase regards the light polarization state as a spin-$1/2$ particle, in contrast to the photon's spin-1, which for example is relevant in spin-orbit interaction of light with a non-straight pathway in space [60, 110, 111]. These non-straight pathways lead to a different geometric phase due to the change in light's momentum direction that was studied by Rytov and Vladimirskii [188, 189]. In this thesis, we will use the terms Pancharatnam-Berry phase and Rytov-Vladimirskii-Berry phase to refer to these two different geometric phases of the light beams.

As an example of the effects of the geometric phases on physical observables, we here review the effect of the Pancharatnam-Berry phase on the refraction of light. A Pancharatnam-Berry phase, unlike the dynamical or Rytov-Vladimirskii-Berry phase is independent from the spatial path that is traversed by light. Therefore, it can change abruptly on a subwavelength scale in space. To illustrate this, let us consider a two-dimensional liquid-crystalline metasurface that acts as a polarizer on an incident light beam that travels between two regions with different refractive indices, as shown in Fig. 1.3. A spatial inhomogeneity on the orientation of the liquid crystal molecules then leads to a spatial variation in the induced Pancharatnam-Berry phase of the incident light beam. The effective optical path between two points A and B is then obtained by $L_{\text{opt}} = \int_A^B \mathbf{k}(\mathbf{r}) \cdot \mathrm{d}\mathbf{r} + \Phi_{r_s}$, where the wavevector $\mathbf{k}$ is spatially dependent on the media's refractive index and Φ_{r_s} is the geometric phase that the light acquires at the incident point r_s to the metasurface. To find the classical path of the light beam one uses Fermat's principle, which can be stated as $\delta L_{\text{opt}} = 0$ with respect to the variations around this classical path. For the situation that is depicted in Fig. 1.3, this leads to the generalized Snell's law of refraction given by [98]

$$k_0 \left[n_t \sin\theta_t - n_i \sin\theta_i \right] = \partial_x \Phi. \tag{1.11}$$

Thus, a spatial change in the geometric phase can affect the refraction of light in a medium. For a Pancharatnam-Berry geometric phase, this effect can take place on a subwavelength scale.

Additional to various examples of geometric phases in classical models, the topological concepts are also well-known in these systems. Liquid crystal disclinations are singularities around which a parallel transport of the director field yields a $\pm\pi$ phase regardless of the path that is taken around them, similar to what happens in the Möbius strip example above. These are examples of topological defects [127, 171]. Such defects also appear in lines of curvature around a degenerate umbilical point on curved surfaces [173], and crystalline defects in solids and mechanical systems [138].

Interestingly, topology in the sense of topological states in integer quantum Hall effect is also found in classical models. The crosspoint lies at the concept of band topology: waves in classical systems, such as light waves in photonic crystals or phonon modes in mechanical systems, have a dispersion relation associated to them, similar to quantum band structure of solids [114, 136]. Thus, one can imagine Chern numbers are being calculated for isolated bands in these wave dispersions as well [82, 109, 113, 115].

1.3 This thesis

We will discuss in this thesis topology and geometric phases of the phonon modes in a metamaterial, the photonic states in an artificial lattice in liquid crystals, and hydrodynamic instabilities in a rotating Rayleigh-Bénard cell.

In chapter two, we consider phonon modes of an elastic metamaterial. For this we consider a simplified model of beads and springs [109]. The vibrational modes of this system are obtained by analysing its linear response around the equilibrium state. It is then possible to start from the Newton's second law for each bead and write down $m\ddot{\mathbf{u}} = D\mathbf{u}$, where D is the dynamical matrix, m is the bead's mass, and $\mathbf{u}$ is the bead's displacement from the equilibrium state. Inspired by Dirac's derivation of the Klein-Gordon equations [193], Kane and Lubensky argued in 2014 in an influential paper that one can take the square root of this equation to get to a Schrodinger equation with a Hamiltonian that is given by [82]

$$H = \begin{pmatrix} 0 & Q \\ Q^{\mathrm{T}} & 0 \end{pmatrix}, \tag{1.12}$$

where Q is called the equilibrium matrix that relates the force applied on the bead i to the spring tensions through [66]

$$F_i = Q_{im} T_m. \tag{1.13}$$

It is then possible to relate the phonon dispersion of the system to the band structure of the Hamiltonian H. In this chapter, we use this connection to quantum mechanics to design a mechanical metamaterial which has a Dirac cone in its band structure. We find an equivalent to a vector potential for the phonon modes that minimally couples to their momentum around the Dirac points in the BZ by applying strain or a variation of the material's local stiffness. We further find the phenomena associated with the presence of this synthetic gauge field, such as Landau levels for sound. We then find that the zeroth Landau level of this system is a specific case of a more general Jackiw-Rebbi-type topological zero mode in our model and define a sublattice polarization to connect our system to this model.

In the third chapter, we consider the propagation of a monochromatic light wave in a liquid crystal medium. Starting from Maxwell's equation, one can derive the Helmholtz wave equations for the electromagnetic wavefunction, considering a transverse electromagnetic (TEM) wave, $\psi = (E_x, E_y)$ as

$$\frac{\partial^2}{\partial z^2}\psi = -(\nabla_\perp^2 + k_0^2 \boldsymbol{\epsilon})\psi, \tag{1.14}$$

where k_0 is the wavenumber in the free space, $\nabla_\perp$ is the spatial gradient in the transverse plane, and $\boldsymbol{\epsilon}$ is the dielectric tensor of the host material. In a so-called paraxial regime, the wave equation above becomes first order along the propagation direction, z and the equation of motion for a monochromatic electromagnetic wave is cast as

$$i\partial_z\psi = -\frac{1}{2nk_0}\nabla_\perp^2\psi - V[\boldsymbol{\epsilon}]\psi, \tag{1.15}$$

where n is the average refractive index, and $V[\boldsymbol{\epsilon}]$ is an effective photonic potential due to the dielectric medium [104, 108]. It then becomes possible to look at the system in this regime as a quantum mechanical problem. In the liquid crystal system that we consider, when the director field's variation in the perpendicular plane is slow, the system is in the paraxial regime. A periodic modulation of the liquid crystal pattern will then map this system to a quantum mechanical problem with a time-periodic Hamiltonian that are studied with Floquet theory [61, 79]. We then show that such Floquet Hamiltonians, when the director field varies adiabatically, can induce Pancharatnam-Berry phases for a light beam. As a result of such spatially varying geometric phase, the light beam becomes transversely confined, leading to *soft light waveguides*. We then use the tools of Floquet theory to obtain the guided modes for more general nematic textures.

In the fourth chapter, we couple these soft electromagnetic waveguides to each other. We show that coupling between these waveguides, also known as coupled mode approximation in optical systems, follow the rules of a semi-classical tunneling picture, establishing an analogy with quantum mechanics in a many-waveguide level. We then develop a tight-binding model for these waveguide interactions. As a result of this model, we present two archetypal example of topological photonics to be realized in liquid crystals: a 1d SSH chain [172] and a 2d Haldane model [151]. Along the way, we develop two recipes to break the effective time-reversal symmetry by merely using the structural degree of freedom. Another result of this chapter is to have a system which has two different kinds of geometric phases: a Pancharatnam-Berry phase to achieve single waveguides and a Berry geometric phase corresponding to the topological band structure.

In the fifth chapter, we consider a rotating Rayleigh-Bénard convection cell. This time, instead of oscillatory waves we consider growing hydrodynamic instabilities that form patterns in this system. The evolution of such a system is described by a nonlinear, but deterministic set of partial differential

equations [140] such as the Swift-Hohenberg model [174]. Formally, such system can be effectively described by

$$\partial_t \psi = \mathscr{N}[\psi], \tag{1.16}$$

where $\mathscr{N}$ is a nonlinear operator and ψ is system's state function. We will focus on the regimes that the final state of the system is a steady-state ordered pattern. The linear stability analysis around this steady state leads to a complex band structure where the real part is the growth rate and the imaginary part is the frequency of the hydrodynamic modes. We apply the insights discussed above to characterize the topology of these bands. In a separate attempt, we then try to sketch a proposal to apply nonlinear geometric phases [10] for studying patterns close to the threshold of the instability transition in this system, where one can use a perturbative method, that is called the amplitude equations approach, to simplify the full nonlinear equations.